Triplet State Characteristics of Higher Fullerenes

Mihály Kállay, Károly Németh, and Péter R. Surján*

Department of Theoretical Chemistry, Eötvös University, H-1518 Budapest 112, POB 32, Hungary

Received: August 21, 1997; In Final Form: December 2, 1997

A theoretical study on the energetics and the structures of lowest triplets of C_{60}, C_{70}, C_{76}, C_{78}, C_{82}, and C_{84} is reported. Excited state geometries, and excitation and phosphorescence energies, as well as Jahn−Teller distortions for degenerate levels were determined. Zero-field splittings of various triplets were evaluated; the signs and magnitudes of the resulting D and E parameters are quite sensitive to the system and to the symmetry of the particular excited state. Atomic spin density distributions are determined for the lowest triplet states.

I. Introduction

Experimental and theoretical characterization of buckminsterfullerene, C_{60}, is well established. This holds for the crystalline forms as well as for the isolated molecule, both in ground and excited electronic states.[1−3] Less is known about the electronic structure of higher fullerenes, especially about their triplet states.

The significance of the lowest triplets is due to their increased lifetimes which make them available for optical[4−11] and electron paramagnetic resonance (EPR)[12−21] experiments. Triplet state properties are often sensitive functions of structural parameters thus providing a great help in the identification and characterization of samples. Besides, triplet excited fullerenes can be utilized in practice as photosenzibilizers and singlet oxygen generators.[22] For C_{60}, properties of the lowest triplet have been targets of several experimental[5−8,12−16,20,21,23] and theoretical[24−27] studies, extending over their location, spin densities, and zero-field splitting (zfs),[12−16,20,21] as well as the triplet−triplet absorption spectra.[4−8] As a consequence of the high symmetry of C_{60} (I_h for the isolated molecule and T_h in crystal), all of its lowest-lying excited states belong to multidimensional irreducible representations, so they are subjected to Jahn−Teller (JT) distortion.[14−16,20,24−27] In particular, the triplet C_{60} molecule was shown to possess D_{5d} symmetry instead of being icosahedral.[15,16,24,25] In contrast, higher fullerenes may have rather low symmetries, and thus they are not always candidates for JT distortion. Among the systems studied in this paper, only the mono-anionized D_{2d} isomer of C_{84} was reported to distort.[28]

For C_{70}, the location of its excited states has been computed,[29,30] determined experimentally,[6,7,9−13,17,23] and zfs of the lowest tiplet was deduced from EPR spectra.[12,13,17] Triplets of smaller fullerenes were also investigated theoretically.[31] To the best of our knowledge, no similar analysis on higher fullerenes has yet been done, though some data are available in the literature on triplet C_{84},[18,19,22] and the experimental[32−37] and theoretical[37−40] singlet optical spectra of several clusters have been published. Spin densities for a few mono-anionized doublet fullerenes were calculated.[28] Since higher fullerenes can exist in several isomeric forms, establishment of the correct structure of every isomer is rather difficult especially when the isomers belong to the same point group, for in this case their NMR, IR, and Raman spectra can be very similar. Therefore, the comparison of experimental and theoretical EPR fine structure parameters, D and E, can be useful as these are very sensitive to the details of molecular geometry.

Recently, there has been an increasing interest in the properties of higher fullerenes. Theoretical characterization of these cages started by listing their possible topological isomers combinatorically.[41] Among the huge number of isomers, one usually selects only those which satisfy the isolated pentagon rule (IPR),[42] as the presence of adjacent pentagons makes the isomers unstable.[43] While C_{60} and C_{70} possess only one single IPR-satisfying structure, several isomers exist for larger fullerenes.[44] Generally, higher fullerenes prefer lower symmetry forms where pentagons are as far as possible.

Simple Hückel theory gives another useful tool for studying the stability of fullerenes. On this basis, three types of electronic structures can be distinguished: closed, open, and pseudo-closed shells.[45] Closed shells with a fully occupied bonding HOMO are stable. Due to fractional occupancies, an open-shell system is degenerate, and thus it can be a candidate for Jahn−Teller distortion. A pseudo-closed-shell molecule has an occupied HOMO but an empty bonding MO lies close to Fermi level. Pseudo-closed-shell molecules frequently get stabilized by geometry distortion. Possible clusters with closed electronic shells can be predicted on the basis of Fowler's leapfrog[42,46] and carbon cylinder[47] principle, or by the "face spiral" method of Manolopoulos et al.[44] combined with a Hückel analysis of the electronic structure.

Following theoretical predictions, experimental characterization of higher fullerenes began in the early 1990s. From the mass spectra, existence of C_{76}, C_{78}, C_{82}, C_{84}, C_{90}, C_{94}, and C_{96} was evident,[32,48,49] though several other clusters gave some minor peaks. Some of the atom numbers did not occur in the spectra at all: C_{62}, C_{64}, C_{66}, C_{68}, C_{72}, C_{74}, and C_{80}. Generally, these are the molecules which do not have closed electronic shells.

The earliest attempt to isolate C_{76} was made in 1991.[32] Its isolation in milligram quantities was attained by Ettl et al.[33] and Kikuchi et al..[49] The structure of this cluster was established by an interplay between theory and experiment. A computer search using the face spiral method resulted two different IPR satisfying isomers.[43] The one with T_d symmetry has an open-shell HOMO; thus it cannot correspond to the experimentally observed molecule. The other, having D_2 symmetry and a pseudo-closed shell, was proposed to be the most likely structure

S1089-5639(97)02739-4 CCC: $15.00
Published on Web 01/30/1998

for C_{76}. The NMR spectrum,[33,49,50] tight-binding molecular dynamics[51,52] calculations, and a quantum chemical calculation at the AM1 level,[33] as well as HF SCF in double-ζ basis set[53] confirmed the chiral D_2 structure of this molecule.

Preliminary theoretical investigations revealed five fullerene cages with 78 atoms which satisfy IPR.[41] There is one D_3 while there are two D_{3h} and two C_{2v} structures. The last two are denoted by C_{2v}-1 and C_{2v}-2, and they can easily be distinguished on the basis of their NMR spectra, because they have 22 and 21 lines, respectively.[41]

The energy order of various isomers was controversial: different theoretical methods predicted different relative stabilities. Only one of the D_{3h} isomers has closed and the others have pseudo-closed shells in qualitative MO theory; more sophisticated quantum chemical calculations predict the relative instability of the D_{3h} isomers. Simple molecular mechanics yields the following stability order: C_{2v}-1 > C_{2v}-2 > D_3 > D'_{3h} > D_{3h}[34] (notations for the D_{3h} isomers can be found therein). Tight-binding simulations also predict the C_{2v}-1 structure to be the most stable one,[51,52] the energy order is C_{2v}-1 < D_{3h} < C_{2v}-2 < D_3 < D'_{3h}. HF SCF/3-21G calculations using MNDO optimized geometry yield the same result as molecular mechanics.[54] Geometry optimization using 3-21G basis set and a subsequent single-point calculation in 6-31G* basis[55] resulted in the energy order C_{2v}-1 < C_{2v}-2 < D_3 < D_{3h} < D'_{3h} (3-21G) and C_{2v}-1 < D_3 < C_{2v}-2 < D_{3h} < D'_{3h} (6-31G*). Niles and Wang carried out Hartree−Fock as well as local density approximation (LDA) calculations.[56] They pointed out that the energy order is not too sensitive to the basis set quality, but it depends mainly on the method.

C_{78} was observed for the first time as a contaminant of C_{76}.[33] Diederich et al.[34] reported the preparation of the mixture of the D_3 and one of the C_{2v} isomers. The latter was assigned to the C_{2v}-2 structure by NMR. Isolation of the C_{2v}-1 isomer was reported by Kikuchi et al.,[57] Taylor et al.,[50,58] and Wakabayashi et al..[59] Formation of the D_{3h} isomers was not observed at any pressure.

C_{82} has nine isomers which satisfy the pentagon isolation rule:[57,60] three C_2, three C_s, two C_{3v}, and one C_{2v}. They are connected by Stone−Wales (SW) transformations[61] only in one family; thus there is supposed to be only one dominant isomer among them. Domination of C_{3v} isomers can be excluded because they have an open-shell HOMO, and C_{2v} structures are stabilized by spontaneous distortion.[62] Detailed experimental characterization of the molecule was given by Kikiuchi and coworkers.[49,57] The NMR spectrum suggests that one of the C_2 structures is the main component. Weaker lines were assigned to C_{2v} and C_{3v} isomers, and the mixture was supposed to contain other C_2 and C_s isomers as contaminant. This is in good agreement with the theoretical results which suggest the three C_2 isomers to be the most stable ones.[52,62] Nevertheless, the anomalous chromatographic behavior of C_{82} makes the formation of C_{3v} isomers possible.[50] These isomers can get stable in endohedral metal−fullerene complexes (e.g. La@C_{82}) where the molecule will have a closed HOMO shell by accepting electrons.[62,63]

Besides C_{60} and C_{70}, the most often investigated fullerene is C_{84}. It was obvious from the first experiments that a 84 atom sized cluster gives a high peak in the mass spectra of carbon soot.[1] Theoretical considerations predicted three isomers by Fowler's rules,[36,42,45,64−66] and altogether 24 IPR satisfying structures were found by the ring spiral algorithm.[42] Among them, the isomers identified by D_2-22 and D_{2d}-23 were proved[67] to be the most stable ones by semiempirical tight-binding[51,52,68] and MNDO[69] calculations.

The first report on the isolation of C_{84} was presented by Diederich et al..[32] It was separated with C_{76} and higher fullerenes (*vide supra*). The molecule gave a relatively sharp line in the mass spectrum but a rather diffuse HPLC profile, consistent with the fact that the sample is composed of two isomers. The structure of the D_2-22 and D_{2d}-23 isomers was confirmed by NMR.[50,57,70] Separation of the two isomers is rather difficult by chromatography because of their high similarity. It was solved, however, by the selective complex formation of the molecules.[71]

The aim of the present paper is to report for a theoretical analysis on the triplet states of C_{60}, C_{70}, C_{76}, C_{78}, C_{82}, and C_{84} clusters. They will be considered in (ground state) isomeric forms C_{60} (I_h), C_{70} (D_{5h}), C_{76} (D_2), C_{78} (D_3, C_{2v}-1, C_{2v}-2), C_{82} (C_2-1, C_2-2, C_2-3), and C_{84} (D_{2d}, D_2). These are the isomers which are predicted to be the most stable ones by theory and were actually isolated in practice. Notations and the detailed structures of each isomer will be referred to along with the reported results in section III. As some of the results on triplet C_{60} and C_{70} were reported previously,[24,26,29,72] these clusters will only be briefly reviewed. To our knowledge, this is the first paper in which triplet states of C_{76} and on are treated theoretically.

II. Methods

A. Model Hamiltonian. Carbon clusters, even as large as C_{84}, are available for sophisticated quantum chemical ab initio[53,56,73] and density functional[56,74,75] calculations if one is merely interested in ground state properties. Treatment of excited states is more demanding computationally, especially if the mixing of several excited configurations is important and/or geometry optimization is needed. Therefore, most successful attempts to describe the excited states of fullerenes were done at some semiempirical level.[24,30,76,77] As we wanted to perform a series of calculations for several clusters in many states, we have applied a very simple model, which, however, was developed to give a reliable account of the properties of low-lying excited states in conjugated systems.[24]

The essence of the model is as follows. Each atom (site) of a cluster contributes one electron and one basis orbital. Only first neighbor sites interact and their interaction is described by the following Hamiltonian:

$$\hat{H} = \sum_{i}^{\text{bonds}} \beta(r_i) \sum_{\sigma} (a^{+}_{i_1\sigma} a_{i_2\sigma} + \text{HC}) - \sum_{i}^{\text{bonds}} \gamma(r_i)(Z_{i_1}\hat{n}_{i_2} + Z_{i_2}\hat{n}_{i_1}) + \sum_{\mu}^{\text{atoms}} \frac{\gamma_\mu}{2}(\hat{n}_\mu^{\,2} + \hat{n}_\mu) + \sum_{i}^{\text{bonds}} \gamma(r_i)\hat{n}_{i_1}\hat{n}_{i_2} + \sum_{i}^{\text{bonds}} f(r_i) + \sum_{i}^{\text{bonds}} \frac{Z_{i_1}Z_{i_2}}{\epsilon r_i} \quad (1)$$

where $a^{+}_{i_1\sigma}$ ($a_{i_1\sigma}$) are electron creation (annihilation) operators obeying Fermion anticommutation rules, i_1 and i_2 are the two sites of bond i, σ is a spin label, and HC means Hermitian conjugate. The $\beta(r_i)$ is the bond length dependent hopping integral having an exponential form: $\beta(r_i) = -A\mathrm{e}^{-r_i/\xi}$, with the length of i-th bond r_i, while A and ζ denote empirical constants. The repulsion of atomic cores and the first-neighbor electron repulsion integrals were parametrized by a Coulombic potential with an effective dielectric constant (ϵ): $\gamma(r_i) = 1/\epsilon r_i$, Z_μ indicates the charge of the μ-th atomic core. The γ_μ stands for

the on-site electron repulsion integrals. The particle number operators $\hat{n}$ are defined as

$$\hat{n}_\mu = \sum_\sigma a^+_{\mu\sigma} a_{\mu\sigma} \tag{2}$$

The potential $f(r_i)$ in eq 1 describes the effect of hidden σ-electrons (*vide infra*). Geometry optimization was carried out on the basis of Coulson's linear bond order−bond length relationship:[78]

$$r_i = r_0 - \kappa P_i \tag{3}$$

where r_0 and κ are empirical parameters, while bond orders are defined as the off-diagonal elements of the first-order density matrix:

$$P_i = \sum_\sigma \langle \Psi | a^+_{i_1\sigma} a_{i_2\sigma} | \Psi \rangle \tag{4}$$

The Coulson rule (3) and the condition of stationarity, $\partial E/\partial r_i = 0$, where E is an eigenvalue of $\hat{H}$, represent a system of differential equations for $f(r_i)$. For the ground state, these are solved by the following potential:

$$f(r_i) = \gamma(r_i)\left(\frac{1}{2}\frac{(r_0 - r_i)^2}{\kappa^2} - q_{i_1} q_{i_2}\right) + 2\beta(r_i)\left(\frac{\zeta}{\kappa} - \frac{r_0 - r_i}{\kappa}\right) + \frac{r_0 \log(r_i) - r_i}{\epsilon\kappa^2} \tag{5}$$

where q_μ are net atomic charges ($q_\mu = Z_\mu - P_{\mu\mu}$).

The model can be solved by the following iterative procedure. Starting from an initial guess of bond lengths, the Hamiltonian of eq 1 is constructed and diagonalized. Having obtained the wave function, bond orders are evaluated from eq 4 and they can be subsequently used to define new bond lengths *via* eq 3. Then, the Hamiltonian is rediagonalized and the procedure is repeated until self-consistency. This method, besides the energies and wave functions, yields an energy-optimized bond length distribution for the desired state.

The electronic part of this Hamiltonian accounts for first-neighbor electron hopping (first term), core−electron attraction (second term), on-site and first-neighbor electron repulsion (third and fourth terms). Accordingly, it corresponds to an extended Hubbard model. Inclusion of electron−phonon coupling through bond length dependent parameters, $\beta(r_i)$ and $\gamma(r_i)$, as well as the core−core repulsion and σ-potential (last two terms of eq 1) makes possible to describe geometry effects. To reflect these features, we refer to this model by the acronym xHUGE (extended *Hu*bbard with *ge*ometry optimization). Originally, the xHUGE model was developed to study excited states of C_{60}.[24,26] A similar model was also used by Fagerström and Stafström.[79] Apart from the treatment of electron interaction, the xHUGE model is closely related to that described by the SSH (Su−Schrieffer−Heeger) Hamiltonian[80] which is physically equivalent to the early model of Longuet−Higgins and Salem,[81] which was recently reparametrized and applied successfully for conjugated polymers in our laboratory.[82,83]

B. Parametrization. The semiempirical parameters of the model were fixed by the following conditions: the energy gap of polyacethylene (1.5 eV), its bandwidth (10 eV), and the lowest singlet and triplet transition energies of the ethylene molecule (7.7 and 4.5 eV). This is achieved by choosing $A = -179.7003$ eV, $\zeta = 0.326288$ Å, $\gamma_\mu = 3.536$ eV, and $\epsilon = 2.24$ (eVÅ)$^{-1}$. We have selected $r_0 = 1.54$ Å (the length of a single C−C bond) and $\kappa = 0.21$ Å by which the length of an unconjugated double C=C bond becomes $r_0 - \kappa = 1.33$ Å. Partially conjugated bond lengths will fall between these two extremes. The reliability of the xHUGE model with this parameter set can be inferred from Table 1.

TABLE 1: Test Calculations by xHUGE Model

molecule	observable[a]	xHUGE	expt	ref
benzene	r	1.40	1.40	120
	$^1\Delta E$	4.9	4.9	121
	$^3\Delta E$	3.7	3.9	122
butadiene	$^1\Delta E$	5.2	5.6	123
naphthalene	$^1\Delta E$	4.0	4.0	124
	r_a	1.426	1.421	120
	r_b	1.378	1.361	120
	r_c	1.432	1.425	120
	r_d	1.419	1.410	120
C_{60}	r_1	1.402	1.40	125
	r_2	1.446	1.45	125
	$^1\Delta E$	2.15	2.0−2.3	126,127
	$^3\Delta E$	1.8	1.6	6,7
thiophene	r(C−S)	1.770	1.718	120
	r_a(C−C)	1.356	1.352	120
	r_b(C−C)	1.425	1.455	120
anthracene	D	0.075	0.072	104
phenanthrene	D	0.092	0.100	104
thiophene				
dimer	D	0.096	0.097	128
trimer	D	0.079	0.078	128
tetramer	D	0.069	0.068	128
pentamer	D	0.063	0.064	128

[a] r denotes bond lengths (Å), $^{1,3}\Delta E$ means the lowest singlet or triplet excitation energy (eV), D is zfs parameter (cm^{-1}).

Application of a one-electron per site model for carbon cages (fullerenes) merits some discussion. Such a model would emerge naturally for a planar system for which the $\sigma-\pi$ separation could fully be maintained, and the hybridization states of atoms would be sp^2. In fullerenes, several hybridization studies[84−87] have shown that the atoms can be described by an intermediate between sp^2 and sp^3. This follows naturally from the curvature of the C_{60} surface. For higher fullerenes, the surface curvature is even smaller, and thus the application of a quasi-π-electron theory is even better justified. Nevertheless, application of quasi-π-electron methods for C_{60} is quite successful,[84,85,88−92] and the data in Table 1 support also that the xHUGE model does a good job for bond length distributions and the energetics of low-lying excited states.

C. Levels of Approximation. Exact solution of the model defined by eq 1 would be tedious. We, therefore, use the following approximate wave functions. The closed-shell *ground state* is approximated by a Hartree−Fock wave function:

$$|\Psi^0\rangle = \psi^+_{1\alpha}\psi^+_{1\beta}\,\psi^+_{2\alpha}\psi^+_{2\beta} \ldots \psi^+_{N\alpha}\psi^+_{N\beta}|\mathrm{vac}\rangle \tag{6}$$

where the molecular orbitals (MOs) ψ^+ are defined variationally. *Excited states* Ψ^J can be defined in several approximations. Of these, two models will be used in this work: Ψ^J can emerge from a configuration interaction (CI) among single excitations relative to the HF ground state (CI-S or Tamm−Dancoff approximation, TDA); alternatively, one can get the HF equations converged directly for the open-shell excited state. If this is done while keeping two electrons with opposite spins on each fully occupied orbital, one has the restricted open-shell Hartree−Fock (ROHF) scheme.[93] As both CI-S and ROHF are standard methods of quantum chemistry, and they will not be reviewed in detail; merely their significance to our model will be discussed below.

The form of the spin adapted triplet CI-S wave function is

$$|^3\Psi^J\rangle = \frac{1}{\sqrt{2}}\sum_{i\to k} C^J_{ik}(\psi^+_{k\alpha}\psi^-_{i\alpha} - \psi^+_{k\beta}\psi^-_{i\beta})|\Psi^0\rangle \tag{7}$$

The CI coefficients C^J_{ik} are determined variationally. In eqs 6 and 7, $\psi^+(\psi^-)$ are creation (annihilation) operators for MOs, which are linear combinations of the atomic site Fermion operators, a^+_μ:

$$\psi^+_i = \sum_\mu c_{i\mu} a^+_\mu \tag{8}$$

Bond orders are evaluated by substituting the relevant wave function into eq 4. We get

$$P^G_i = 2\sum_k^{\text{occ}} c_{ki_1} c_{ki_2} \tag{9}$$

for the ground state, and

$$P^J_i = P^G_i - \sum_{jk}^{\text{occ}}\sum_{l}^{\text{virt}} C^J_{jl}C^J_{kl}c_{ji_1}c_{ki_2} + \sum_{j}^{\text{occ}}\sum_{kl}^{\text{virt}} C^J_{jk}C^J_{jl}c_{ki_1}c_{ki_2} \tag{10}$$

for the excited state J, where $c_{i\mu}$ are the LCAO and C^J_{ij} are the CI coefficients.

Solution of the above model requires a double iteration procedure. An SCF iteration is performed to get the self-consistent Hartree−Fock (HF) solution at the given set of bond lengths. The CI is done on the top of HF, and the excited state bond orders are evaluated through eq 10. Then, bond lengths are optimized in an outer loop as described before.

The most time-consuming step in the xHUGE-CI procedure is the variational optimization of the CI coefficients C^J_{ik} in eq 7 which requires repeated diagonalization of large matrices. This can turn infeasible for large clusters very soon. Another disadvantage of this procedure is that the form of the σ-potential, $f(r_i)$ of eq 5, was derived for the ground state, and the accurate excited state version of $f(r_i)$ cannot be put down analytically in the CI-S model. Therefore, we have also determined the lowest triplets by optimizing the one-electron MOs directly for these states, in the spirit of Roothaan's ROHF procedure.[93] Accordingly, the $S_z = 0$ triplet wave function is written as

$$|^{3,0}\Psi^J_{\text{ROHF}}\rangle = \frac{1}{\sqrt{2}}(\varphi^+_{\text{L}\alpha}\varphi^-_{\text{H}\alpha} - \varphi^+_{\text{L}\beta}\varphi^-_{\text{H}\beta})|\Psi^0_{\text{ROHF}}\rangle \tag{11}$$

where H (L) stand for HOMO (LUMO), and $|\Psi^0_{\text{ROHF}}\rangle$ has the same structure as that of $|\Psi^0\rangle$, but it is built up from the excited state orbitals φ. It is apparent from eq 11 that it gives a two-determinantal wave function for the $S_z = 0$ triplet due to spin adaptation. The equations for the orbitals φ can be found in the classical paper by Roothaan.[93]

The wave function for the $S_z = 1$ triplet is written as

$$|^{3,1}\Psi^J_{\text{ROHF}}\rangle = \varphi^+_{\text{L}\alpha}\varphi^-_{\text{H}\beta}|\Psi^0_{\text{ROHF}}\rangle \tag{12}$$

The atomic spin densities at site μ corresponding to the above wave function are easily evaluated as

$$\rho^{\text{spin}}_\mu = \langle^{3,1}\Psi^J_{\text{ROHF}}|a^+_{\mu\alpha}a_{\mu\alpha} - a^+_{\mu\beta}a_{\mu\beta}|^{3,1}\Psi^J_{\text{ROHF}}\rangle \tag{13}$$

The ROHF bond orders P_i have a closed-shell and an open-shell contribution:

$$P_i = P^{\text{closed}}_i + P^{\text{open}}_i \tag{14}$$

where

$$P^{\text{closed}}_i = 2\sum_k^{\text{closed}} c_{ki_1}c_{ki_2} \tag{15}$$

$$P^{\text{open}}_i = c_{\text{H}i_1}c_{\text{H}i_2} + c_{\text{L}i_1}c_{\text{L}i_2} \tag{16}$$

The ultimate advantage to combine the ROHF scheme with the xHUGE model is that the σ potential $f(r_i)$ can be derived directly for the excited state. Combining the Coulson formula eq 3 with the stationary condition

$$\partial E/\partial r_i = 0$$

with E now being

$$E = \langle^3\Psi^J_{\text{ROHF}}|\hat{H}|^3\Psi^J_{\text{ROHF}}\rangle$$

one gets

$$f_{\text{ROHF}}(r_i) = f(r_i) + {}^1/_2\gamma(r_i)P^{\text{open}}_i \tag{17}$$

where $f(r_i)$ has the same expression as in eq 5.

Direct comparison of the CI-S and ROHF wave functions is not straightforward as they are defined over a different set of one electron MOs, ψ_i and φ_i, respectively. As it is apparent from eq 7, the CI-S wave function consists of a large number of determinants in the ψ basis, while Ψ_{ROHF} corresponds to a single configuration (cf. eqs 11 and 12) in the φ space. The question of the multiconfigurational structure of $\Psi_{\text{CI-S}}$ is very important to judge the extent of electron correlation described. The problem is nontrivial as the excited state $\Psi_{\text{CI-S}}$ is composed of MOs which were optimized for the ground state. An unambiguous tool to investigate the electron correlation exhibited by some wave function is offered by the expansion in terms of natural orbitals.[94] These are the orbitals which diagonalize the first-order density matrix P. The eigenvalues of this matrix are interpreted as generalized occupation numbers. An integer eigenvalue does not, and a fractional does, indicate a truly multiconfigurational behavior. Moreover, the natural MOs have the property that they support the fastest possible convergence of the CI expansion. Therefore, an analysis of the CI convergence in terms of natural orbitals offers a valuable information about the electronic structure. Such an analysis will be reported in this paper for C_{60} and C_{70}.

D. Handling of Degeneracies and Jahn−Teller Distortion. Optimization of the above method is straightforward if the molecule in question belongs to an Abelian group; that is, no degenerate levels can be expected in the spectrum. If, however, there are multidimensional degenerate one-electron states at around the Fermi level, special attention should be paid to constructing the appropriate many-electron wave function. Failure to do so will almost certainly lead to convergence difficulties either in the SCF or in the geometry optimization procedure, or both, as well as to an unphysical solution. Among the clusters studied in this paper, this problem is topical for C_{60}, C_{70}, and C_{78}. The problem can be automatically handled with the aid of group theory. The aim is to produce density matrices (e.g., bond orders P_i) which exhibit a definite symmetry even if the wave function they result from (cf. eq 4) is degenerate. By the term "definite symmetry" we mean an irreducible representation in one of the subgroups of the parent

point group. Among all subgroups, one has to select those to which a Jahn−Teller distortion[95−98] may take place. Then, unique density matrices can be obtained by reducing the many-electron wave function to the desired one-dimensional representation of a subgroup. We do this by standard group theoretical projection techniques:

$$|\Psi^{\Gamma}\rangle = \sum_{\hat{R}} \chi_{\Gamma}(\hat{R})\hat{R}|\Psi^{J}\rangle \tag{18}$$

where Ψ^{Γ} is the (unnormalized) wave function reduced to the subgroup irreducible representation Γ, $\hat{R}$ runs over the symmetry operations of the selected subgroup, and $\chi_{\Gamma}(\hat{R})$ is the character of the element $\hat{R}$, while Ψ^{J} is the original multidimensional parent wave function. Computing the density matrix by Ψ^{Γ} instead of Ψ^{J} leads to unique symmetry-adapted bond orders corresponding to a desired state, the use of which yields optimum geometries distorted into the selected subgroup.

The Jahn−Teller distortion energies are defined by

$$\Delta E_{JT} = E_J^{\Gamma} - E_J^0 \tag{19}$$

where E_J^{Γ} is the energy of the distorted state and E_J^0 means the energy of the vertically excited degenerate "parent" representation. This definition does not care for the exited state relaxation energy within the parent group, which is, as we have checked in some cases, a negligible contribution.

E. Zero-Field Splitting. Having obtained the excited structures, we can analyze the triplets as to their zero-field-splitting parameters which are commonly derived from EPR spectra by extrapolating to zero magnetic field.[99,100] The two fundamental parameters D and E, originating from spin−spin interaction, are defined theoretically in the laboratory principal axis coordinate system as[99]

$$D = \frac{3}{4}g^2\beta^2\left\langle {}^3\Psi\left|\sum_{i<j}\frac{x_{i,j}^2 + y_{i,j}^2 - 2z_{i,j}^2}{r_{i,j}^5}\right|{}^3\Psi\right\rangle \tag{20}$$

$$E = \frac{3}{4}g^2\beta^2\left\langle {}^3\Psi\left|\sum_{i<j}\frac{x_{i,j}^2 - y_{i,j}^2}{r_{i,j}^5}\right|{}^3\Psi\right\rangle \tag{21}$$

where the summation indices i, j run over all electrons, $g = 2.002\,32$ is the free-electron g factor, and $\beta = e\hbar/2m$ is the Bohr magneton. Physically, D means the zero-field energy difference between the $|\pm1\rangle$ and $|0\rangle$ components of the triplet state, while $2E$ is the splitting between the $|+1\rangle$ and $|-1\rangle$ levels.

Using eqs 7 and 8 (or their ROHF analogues) for the triplet state wave function, the calculation of the parameters D and E reduces to the evaluation of the respective two-electron integrals between atomic orbitals. Since our theory is based on a one-orbital-per-site model, we may assume that the underlying AOs are quasi π-type hybrids which are directed perpendicular to the surface of the cluster.[87,88,101] However, because we use a semiempirical technique to handle these integrals, too, we do not need to specify these orbitals explicitly.

The general integrals over AOs χ take the form

$$\left\langle \chi_{\mu}(1)\chi_{\nu}(1)\left|\frac{\xi_{1,2}^2}{r_{1,2}^5}\right|\chi_{\lambda}(2)\chi_{\rho}(2)\right\rangle \tag{22}$$

where ξ stands for x, y, and z which are defined in the symmetry axis coordinate system. Under the zero-differential-overlap (ZDO) approximation[102] only the following integrals survive:

$$\left\langle \chi_{\mu}^2(1)\left|\frac{\xi_{1,2}^2}{r_{1,2}^5}\right|\chi_{\lambda}^2(2)\right\rangle \tag{23}$$

In fact, these are the dominating integrals.[103]

In semiempirical theories the ZDO condition is used together with the so-called spherical approximation to maintain the rotational invariance of the results.[102] This means that no distinction is made among p_x, p_y, and p_z type orbitals in two-electron integrals. In particular, the integrals $\langle\chi^2|x^2/r^5|\chi^2\rangle$, $\langle\chi^2|y^2/r^5|\chi^2\rangle$, and $\langle\chi^2|z^2/r^5|\chi^2\rangle$ are all the same. Consequently, no one-center term in eq 23 can have a contribution to D or E, and one has to deal merely with two-center integrals.

Transforming these integrals from the symmetry frame to the local coordinate system, one arrives at the following two types of expressions:

$$\left\langle \chi_{\mu}^2(1)\left|\frac{x'^2_{1,2}}{r_{1,2}^5}\right|\chi_{\lambda}^2(2)\right\rangle \tag{24}$$

$$\left\langle \chi_{\mu}^2(1)\left|\frac{z'^2_{1,2}}{r_{1,2}^5}\right|\chi_{\lambda}^2(2)\right\rangle \tag{25}$$

where the primed coordinates refer to the local coordinate system and where the interatomic axis is z'. Equation 24 is a locally π-type integral while eq 25 is of type σ. In the spherical approximation these integrals depend merely on the distance R between atoms μ and λ. The π-type integrals fall off as R^{-5}, while the σ integrals decrease asymptotically as R^{-3}. Accordingly, we have parametrized them by

$$\left\langle \chi_{\mu}^2(1)\left|\frac{x'^2_{1,2}}{r_{1,2}^5}\right|\chi_{\lambda}^2(2)\right\rangle = \frac{I_{\pi}}{R^5} \quad \text{and} \quad \left\langle \chi_{\mu}^2(1)\left|\frac{z'^2_{1,2}}{r_{1,2}^5}\right|\chi_{\lambda}^2(2)\right\rangle = \frac{I_{\sigma}}{R^3} \tag{26}$$

where I_{σ} and I_{π} are new empirical parameters. For I_{π}, we used different values in the D and E integrals, denoted by I_{π}^D and I_{π}^E, respectively. These parameters have been fitted to reproduce $D = 0.15$ cm^{-1} for D_{6h} benzene,[104,105] and the experimental results $D = 0.099$ cm^{-1} and $E = 0.015$ cm^{-1} for naphtalene.[104,106] The corresponding values, including the constant $^3/_4g^2\beta^2$ in eqs 20 and 21, are $I_{\pi}^D = 5.303\,34$ cm^{-1} Å^5, $I_{\pi}^E = 4.279\,38$ cm^{-1} Å^5, and $I_{\sigma} = 3.336\,87$ cm^{-1} Å^3.

Evaluation of the above integrals requires the knowledge of atomic coordinates. The xHUGE model defined in section IIA yields optimized bond lengths only. Cartesian coordinates of all atoms have been obtained by maximizing all interatomic distances subject to the condition that optimal bond lengths are preserved. This procedure was shown to provide good 3D geometries for rings[107] and hollow cages.[25,29]

III. Results and Discussion

Usually, EPR experiments see the lowest triplet state, but the spectrum can be affected by higher triplets. Therefore, we examined the lowest three or four triplet energy surfaces of the clusters. After a short summary of previous results on C_{60} and C_{70}, augmented with some recent findings, we deal with the isolated isomers of higher fullerenes. The results are collected in Tables 2−12. In the first row of each table the ground state

TABLE 2: Ground and Excited State Parameters for C_{60}

group	state	parent rep	total energy (eV)	ΔE_{JT} (MeV)	D (cm^{-1})	E (cm^{-1})
ground state						
I_h	$^1A_{1g}$		−1374.057			
CI						
D_{5d}	$^3A_{2g}$	T_{2g}	−1372.352	−185	−0.010	0
	$^3A_{1g}$	H_g	−1372.075	−28	−0.007	0
	$^3A_{2u}$	T_{1u}	−1371.573	−20	−0.058	0
	$^3A_{1u}$	H_u	−1371.461	−3	0.018	0
T_h	^3A_g	G_g	−1371.982	−3	0.000	0
	^3A_u	G_u	−1371.611	−5	0.000	0
D_{3d}	$^3A_{2g}$	T_{2g}	−1372.226	−59	0.008	0
	$^3A_{1g}$	H_g	−1372.057	−10	0.009	0
	$^3A_{2u}$	G_u	−1371.649	−43	−0.021	0
	$^3A_{1u}$	G_u	−1371.617	−11	0.038	0
D_{2h}	$^3B_{1g}$	T_{2g}	−1372.287	−120	−0.019	0.000
	^3A_g	H_g	−1372.059	−12	0.013	0.004
	$^3B_{1u}$	G_u	−1371.668	−62	0.031	0.002
	^3A_u	H_u	−1371.641	−183	0.014	0.004
ROHF						
D_{5d}	$^3A_{2g}$	T_{2g}	−1372.305		0.001	0

energies are given, so one can compare the stabilities of isomers predicted by our model. Subsequent rows correspond to the results of all-single-CI calculations for the lowest triplet potential surfaces. At the bottom of the tables, the ROHF energy and zfs parameters are shown for the lowest triplet. For Jahn−Teller active cases we give the "parent representation" for each distorted state, which is the irreducible representation from which the molecule distorts. If the zfs E value is zero by symmetry we indicate it putting "0". In Table 13, predictions for the zfs measurements for all examined systems are summarized. Characterization of critical points (minima *vs* saddle points) was based on calculating Hessian eigenvalues. These are not included in the tables but will be mentioned in course of the discussion for each relevant case. We do not tabulate phosphorescence energies but they will also be mentioned in the text for each isomer. Geometries for ground and excited states have been determined. They will not be tabulated either but are available from the authors upon request.[108]

A. C_{60}. It is well-known[24,89] that all low-lying excited states of buckminsterfullerene, C_{60}, belong to a multidimensional irreducible representation of the I_h group. Therefore, though the ground state molecule is icosahedral, a loss of spatial symmetry will take place in excited states due to Jahn−Teller distortion. The energetics and geometry of Jahn−Teller distorted states were presented previously,[24] and the zfs D value of the lowest triplet was also given.[72] The results are summarized in Table 2. The experimental zfs results[4,13,14,72] are $|D| = 0.011$ cm^{-1} and $E \approx 0$, the sign of D is unknown. These parameters agree with those calculated for the $^3A_{2g}$ state where the cluster is distorted into D_{5d} symmetry. This state is indeed the lowest triplet, it has the largest Jahn−Teller distortion energy (−185 meV), and it is the only minimum on the lowest triplet potential surface. All other critical points are saddles, including $^3B_{1g}$ in D_{2h} which is the second lowest triplet. Distortion in the D_{5d} $^3A_{2g}$ state is demonstrated in Figure 1a.

There is another critical point on one of the higher surfaces, $^3A_{1g}$ in D_{3d}, possessing a zfs pattern ($|D| = 0.009$ cm^{-1} and $|E| = 0$ cm^{-1}) which would be also in agreement with the experimental data, but it is situated by about 300 meV above the lowest triplet.

The JT energy of the triplet minimum ($^3A_{2g}$ in D_{5d}) is quite large, it is much higher than kT at room temperature. According to the six possible C_5 axes in C_{60} which can be preserved also after JT, there are six equivalent JT structures in D_{5d}. The molecule may undergo a pseudorotation among these structures if the barrier is not too high (dynamic JT effect). Using the method of Stachó et al.,[109−111] we have determined the reaction pathway from one minimum to another, and we have shown[27] that the transition states are just the D_{2h} saddle points of ^3A_g symmetry, given in Table 2. We found that the barrier along this pathway is 16 meV (185 K in temperature units). This shows that the thermal motion itself cannot perform the rotation at low temperatures, in accordance with the proposal of Bennati et al.,[15,16] which was based on EPR spectrum simulations.

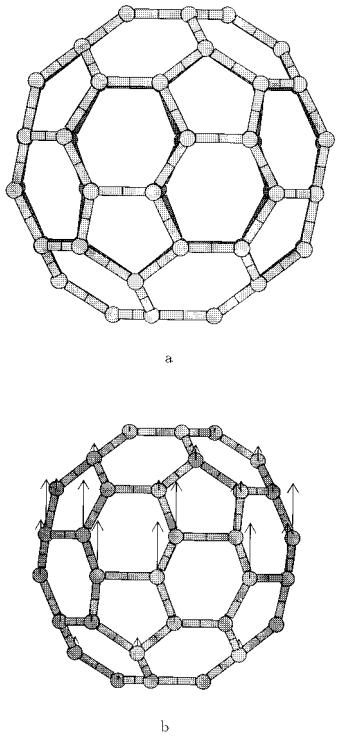

Figure 1. C_{60} molecule (a) Ground state (light) and JT distorted D_{5d} $^3A_{2g}$ excited state geometry (dark). Distortions are magnified for visualization. (b) Atomic spin densities in D_{5d} $^3A_{2g}$ lowest excited state (arbitrary units).

A deeper insight into the electronic structure of triplet states can be obtained by analyzing atomic spin density data. Spins mainly appear on sites where the excitation is localized. Figure 1b depicts atomic spin densities for the triplet ground state and clearly shows an equatorial distribution. (Here and further on in this work, we use the term "equator" for the plane perpendicular to the main rotation axis of the distorted system.) As is seen from eqs 20−21, D measures the deviation of the excitation from spherical symmetry, while E measures the deviation from the cylindrically symmetric case. The simplest model yielding a negative sign for D should have small spin densities in the equatorial space of the C_5 axis in molecules of D_{5d} point group. Of course the atomic position distribution also has an effect in the sign of D. In fact, the equatorial spins are large for the triplet minimum, but this is overcome by the effect of the atomic distribution: the principal axis inertial moment of the molecule is smaller for the C_5 axis than for the other two perpendicular axes. This tells us that simple models based merely on spin density data can be incorrect in the determination of the sign of D.

An interesting feature of the electronic structure of the C_{60} molecule is stressed by the fact that the ROHF and the CI results are very different for this molecule. This is because the ROHF wave function consists of a single configuration, while in our CI calculations all of the singly excited states were allowed to

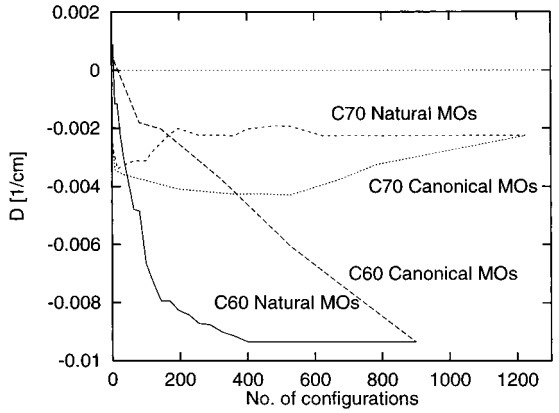

Figure 2. Dependence of zfs D on the size of CI for C_{60} and C_{70}. Plots end at the all-single-CI (900 configurations for C_{60} and 1225 for C_{70}).

interact. Consequently, the CI wave function is capable of describing a significant part of electron correlation which is indicated by the difference between ROHF and CI results.

Direct comparison of the CI and ROHF states is complicated as they are obtained in different sets of MOs: the CI is ground-state-optimized while ROHF is optimized for the excited state. Therefore, to resolve any ambiguity, we have performed CI calculations with an increasing number of configurations both in the basis set of HF MOs and in terms of natural orbitals. The convergence of the zfs D value as a function of the size of CI is shown in Figure 2. It is seen that if one applies only a few number of configurations, one gets the wrong sign for D, just as in the ROHF case. This holds both for HF and natural orbitals. As the number of configurations increases, the results slowly converge to the exact (all-single-CI) value, the convergence being much faster if natural orbitals are used. In this latter case, the lowest number of configurations which provide a good guess to the zfs parameter is about 400, *ca.* half of the possible total number of singly excited determinants in a π-electron calculation of C_{60}. This means that this system is highly correlated in its excited state, and no meaningful wave function can be put down for its triplets below 400 configurations. This feature is peculiar to C_{60}, and as will be shown below, C_{70} and higher fullerenes can be described reasonably by much simpler wave functions.

B. C_{70}. For the triplet state of C_{70}, many experimental results are available.[7,9,12,13,23] Several calculations were also performed to obtain the ground state equilibrium geometry of this molecule at different levels of theory.[66,112−116]

Previous quantum chemical calculations on the spectra of C_{70}[30,117] were limited mainly to singlet excitations. Feng et al.[117] examined the singlet spectrum by semiempirical INDO/CI method. Bendale et al.[30] reported the allowed singlet levels using INDO/CI and RPA methods.

We studied the three lowest triplet states of C_{70} (see Table 3). The lowest triplet is nondegenerate belonging to the A'_2 representation of the D_{5h} point group. The geometry of this state was reported previously.[29] Its vertical excitation energy by the xHUGE model was 1.44 eV at the ground state geometry and it decreased to 1.05 eV upon relaxation in the excited state. The calculated D parameter is quite small, -0.002 cm^{-1}, while E is zero by symmetry. EPR experiments for C_{70} yield smaller D than for C_{60}: $|D| = 0.0052$ cm^{-1} and $|E| \approx 0$.[12,13] The sign of D was supposed to be negative by Closs et al.[13] assuming a spherical spin density distribution. This sign is confirmed by the calculations, although the spin distribution[29] is equatorial as for C_{60}. The absolute value of the experimental D parameter is larger than the calculated one, but both values are rather small, and they are in the accuracy limits of our method (the third decimal in cm^{-1}).

TABLE 3: Ground and Excited State Parameters for C_{70}

group	state	parent rep	total energy (eV)	ΔE_{IT} (meV)	D (cm^{-1})	E (cm^{-1})
ground state						
D_{5h}	$^1A'_1$		−1603.067			
CI						
D_{5h}	$^3A'_2$		−1601.824		−0.002	0
C_{2v}	$^3A_1$	E'_1	−1601.598	−106	−0.032	0.007
	$^3B_1$	E'_1	−1601.598	−106	−0.032	0.007
	$^3A_1$	E'_1	−1601.451	−103	0.005	0.001
	$^3B_1$	E'_1	−1601.451	−103	0.005	0.001
ROHF						
D_{5h}	$^3A'_2$		−1601.791		−0.002	0

Single-configuration ROHF results for state $^3A'_2$ are practically the same as those obtained by the CI-S wave function. Convergence of the computed D value with the size of CI is shown in Figure 2. As compared to C_{60}, the D values vary within a much narrower range and do not change sign when the number of configurations increases. The difference between the convergence properties when natural MOs or canonical HF MOs are used is also smaller, though, of course, natural orbitals provide the optimal convergence. The fact that the quality of the natural MO expansion is not too sensitive to the number of configurations means that the lowest triplet wave function of C_{70} is dominated by a single configuration. This, altogether, indicates a minor role of electron correlation in this system.

The second and third lowest triplets occur in the xHUGE calculation at vertical transition energies 1.57 and 1.72 eV, respectively. Both belong to the E'_1 representation of D_{5h}. The E'_1 states, being degenerate, are subject to a Jahn−Teller distortion from D_{5h} to C_{2v}.[98] The possible irreps (irreducible representations) for the distorted wave function are given by the decomposition of E'_1 as a reducible representation in C_{2v}:

$$E'_1 = A_1 \oplus B_1$$

Reducing the triplet wave function by the relevant projection operator in course of the geometry optimization process results in C_{2v} distorted states A_1 and B_1 shown in Table 3. It is interesting to note that the energy of A_1 and B_1 distorted states do not split significantly after Jahn−Teller distortion and remain quasi-degenerate to three decimals, although their geometries are different. The corresponding zfs parameters are also very close to each other, indicating a similar distortion. Though the surface is quite flat along one of the normal coordinates, all states represent minima on the energy hypersurface, which is a difference from the case of C_{60} where one meets saddle points as well. The calculated Jahn−Teller energy is about 100 meV which falls in the same order as for C_{60}.[24] Due to the distortion the energy of the $T_2 \rightarrow S_0$ (C_{2v} $^3A_1 \rightarrow D_{5h}$ $^1A'_1$) and $T_3 \rightarrow S_0$ (C_{2v} $^3A_1 \rightarrow D_{5h}$ $^1A'_1$) vertical transitions decrease to 1.37 and 1.53 eV, respectively. The order of excited states does not change due to Jahn−Teller distortion.

C. C_{76}. Above C_{70}, the smallest cage we have investigated in this work is C_{76}. As mentioned in the Introduction, this cluster has been isolated and several of its properties have been described. As to the ground state geometry, only theoretical results are available. The bond lengths obtained by ab initio HF calculations in STO-3G basis set vary from 1.36 to 1.49 Å.[53] This range extends to 1.37−1.47 Å according to semiempirical AM1 calculations,[33] to 1.41−1.53 Å in LDA,[75] and to 1.392−1.491 in QCFF/PI[38] calculations. With our model, which

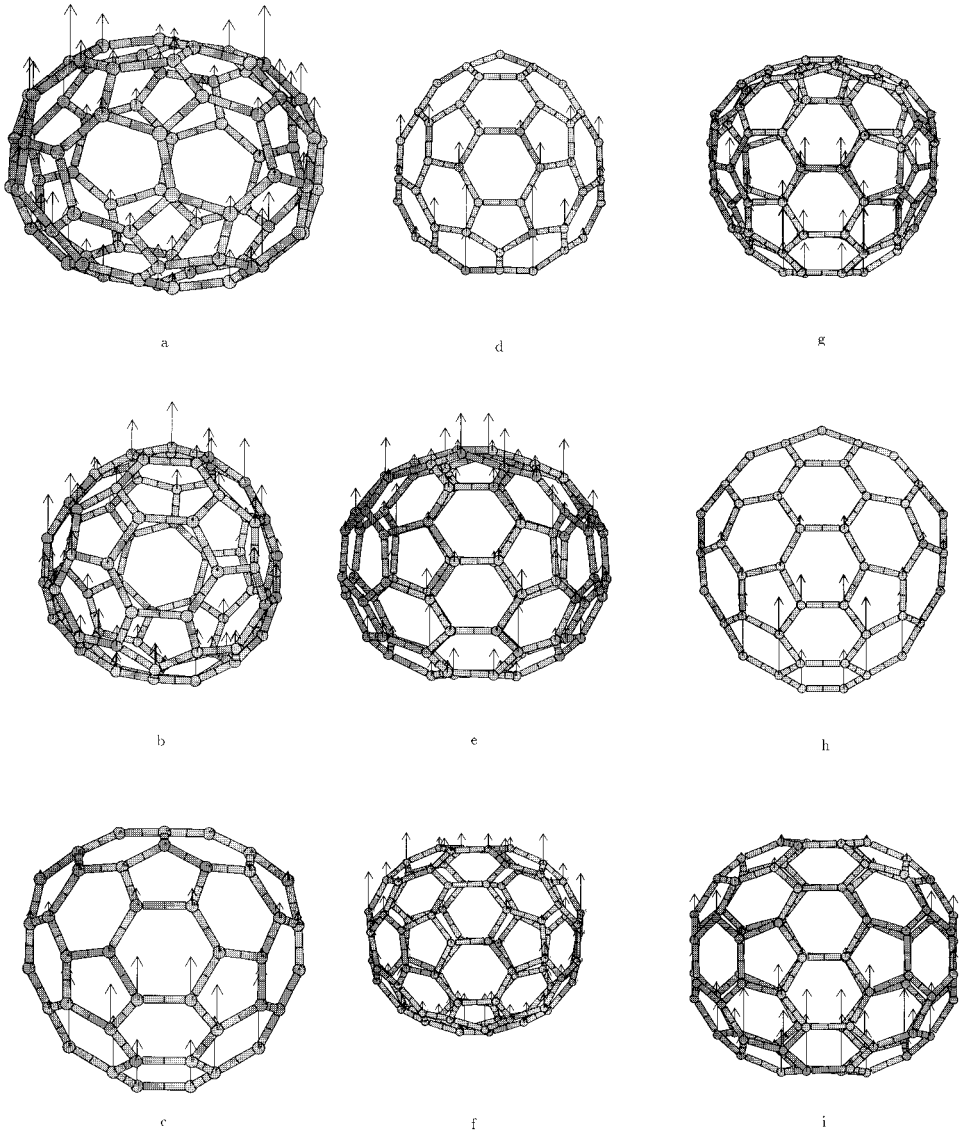

Figure 3. Atomic spin densities in lowest excited states of fullerenes (arbitrary units): (a) C_{76} (D_2), (b) C_{78} (D_3), (c) C_{78} (C_{2v}-1), (d) C_{78} (C_{2v}-2), (e) C_{82} (C_2-1), (f) C_{82} (C_2-2), (g) C_{82} (C_2-3), (h) C_{84} (D_{2d}), (i) C_{84} (D_2).

is supposed to be quite accurate for bond lengths, this interval is 1.399−1.454 Å, tighter than any other results.

The UV/vis spectrum of dissolved C_{76} was published first by Diederich et al..[32] A more detailed optical spectrum was presented by Ettl et al..[33] The lowest maximum occurs at 1.63 eV, but from the absorption onset the band gap is estimated as 1.37 eV.[35,38] It is in agreement with our calculated singlet spectra: we found that there are two transitions with relatively small oscillator strengths at 1.22 and 1.43 eV and there is a maximum at 1.53 eV. In contrast, the lowest singlet excitation energy was predicted to be 1.5 eV by AM1,[33] 1.73 eV by QCFF/PI,[38] 1.2 eV by tight-binding,[40] and 1.1 eV by DFT calculations.[75] It was declared to be a B_3 transition[38] which is opposite to our B_2 assignation.

The triplet state characteristics for this cluster are collected in Table 4. Because the D_2 point group is Abelian, JT distortion cannot occur at any excited states. The excitation energy of the $S_0 \rightarrow T_1$ vertical transition is 1.092 eV which decreased to 0.734 eV upon geometry relaxation in the excited state (the energy of the $T_1 \rightarrow S_0$ vertical transition). The lowest triplet can be assigned as B_2 and characterized as a minimum on the lowest triplet surface by ROHF calculation. Its bond lengths fall between 1.400 and 1.451 Å; that is, the geometry does not change significantly as compared to the ground state. The zfs D parameter is close to that of C_{60}, but we obtained a minor E value which does not necessarily vanish in the D_2 point group. Spin densities in B_2 lowest triplet are shown in Figure 3a, where the molecule can be seen parallel to $C_2(z)$ axis. The spin density distribution is not equatorial as in the case of C_{60}.

TABLE 4: Ground and Excited State Parameters for C_{76}

group	state	total energy (eV)	D (cm^{-1})	E (cm^{-1})
ground state				
D_2	^1A	−1740.547		
CI				
D_2	$^3B_2$	−1739.639	−0.008	0.002
	$^3B_3$	−1739.382	0.016	0.000
	$^3B_1$	−1739.228	0.008	0.000
	$^3B_3$	−1739.212	0.002	0.001
ROHF				
D_2	$^3B_2$	−1739.617	−0.007	0.001

Comparing ROHF and CI-S results for the lowest triplet, we can see a minor difference but not the large discrepancy exhibited by C_{60}.

Higher triplets have either $^3B_3$ or $^3B_1$ symmetries in D_2. The two $^3B_3$ states can easily be distinguished by their D values as

TABLE 5: Ground and Excited State Parameters for C_{78} (C_{2v}-1)

group	state	total energy (eV)	D (cm^{-1})	E (cm^{-1})
ground state				
C_{2v}	$^1A_1$	−1786.471		
CI				
C_{2v}	$^3A_2$	−1785.578	0.020	0.000
	$^3B_2$	−1785.332	−0.009	0.001
	$^3B_1$	−1785.144	−0.021	0.004
	$^3B_2$	−1784.998	0.007	0.003
ROHF				
C_{2v}	$^3A_2$	−1785.556	0.020	0.003

these differ almost by an order of magnitude. The E values of all states remain extremely small.

We have also checked the *spatial transition moments*, i.e., the $\langle T_1|\mathbf{r}|S_0\rangle$ matrix element without spin integration. Their magnitudes are connected to the singlet−triplet transition probability which affects the radiative decay rate of the triplet levels. (They are not given in the tables as we do not claim that our model is sufficiently accurate for a property like this.) These integrals vanish for symmetry reasons in the case of the lowest triplets of C_{60} and C_{70}, but not for C_{76}. Accordingly, the radiative decay rate of C_{76} is expected to be larger than those of C_{60} and C_{70}. However, among the four lowest triplets of C_{76}, the smallest spatial transition moment was obtained for the first state.

D. C_{78}. We investigated the three isolated forms of C_{78}: two C_{2v} and one D_3 isomer.[34,57−59] We use the notation of ref 118 for the isomers. Schlegel diagrams of the five IPR satisfying isomers are shown therein. C_{2v}-1 is equivalent to the molecule exhibiting 22 NMR lines it was noted by number 5 in the original publication of Fowler et al.[41] and by C'_{2v} by Diederich et al..[34] C_{2v}-2 has 21 NMR lines and it was noted by number 4 and C_{2v} by the above authors, respectively.

The energy order in our work is C_{2v}-1 < D_3 < C_{2v}-2 with 0, 82, and 534 meV relative stabilities. The same order comes from HF/6-31G* calculations.[34,51,52,54−56] Relative stabilities obtained with several semiempirical and ab initio calculations can also be found.[54,56]

The bond lengths varied between 1.399 and 1.454, 1.394 and 1.460, and 1.392 and 1.463 Å in our work for the D_3, C_{2v}-1, and C_{2v}-2, respectively, whereas in MNDO calculations[54] average bond lengths were 1.448, 1.447, and 1.448 Å. At HF/STO-3G level the bond lengths were between 1.358 and 1.495, 1.342 and 1.490, and 1.346 and 1.485, respectively.[56] Bond lengths obtained with gradient-corrected DFT calculations were between 1.414 and 1.505, 1.405 and 1.507, and 1.409 and 1.505, respectively.[56] Our values are closer to the HF calculations but the range of the latter is wider which is general for all of the studied systems. This can be attributed to the fact that HF overestimates the bond length alternation.[119]

The optical spectra of the C_{2v}-2 and the D_3 isomers were published.[34] Bendale and Zerner[39] presented the detailed theoretical UV spectra of the C_{78} isomers obtained by the semiempirical INDO/S method. We do not aim to discuss singlet spectra here but just note that our vertical singlet excitation energies are significantly smaller that those in ref 39.

The lowest triplet state of the C_{2v}-1 isomer has A_2 symmetry, cf. Table 5. Its excitation energy is 1.125 eV which decreases to 0.667 eV upon geometry relaxation. Bond lengths fall between 1.401 and 1.451 Å. It is a minimum on the potential energy surface. The $S_0 \rightarrow T_1$ transition is spatially forbidden, therefore its radiative decay rate may be comparable to that of C_{60} and C_{70}. In Figure 3c the isomer can be seen from a view perpendicular to the C_2 axis. It has an interesting spin density distribution: the spins are localized on one half of the cage. The molecule has very strong zero-field splitting: the absolute value of D of this state is about twice as large as that of C_{60}, and its sign is opposite. This is the largest D value we have found for fullerenes up to this time.

TABLE 6: Ground and Excited State Parameters for C_{78} (D_3)

group	state	parent rep	total energy (eV)	ΔE_{JT} (meV)	D (cm^{-1})	E (cm^{-1})
ground state						
D_3	$^1A_1$		−1786.388			
CI						
D_3	$^3A_2$		−1785.667		−0.012	0
C_2	^3A	E	−1785.129	−101	0.019	0.006
	^3B	E	−1785.128	−100	0.019	0.006
	^3A	E	−1785.018	−87	0.007	0.003
	^3B	E	−1785.018	−87	0.007	0.003
ROHF						
D_3	$^3A_2$		−1785.647		−0.008	0

TABLE 7: Ground and Excited State Parameters for C_{78} (C_{2v}-2)

group	state	total energy (eV)	D (cm^{-1})	E (cm^{-1})
ground state				
C_{2v}	$^1A_1$	−1785.937		
CI				
C_{2v}	$^3B_1$	−1785.357	−0.010	0.001
	$^3A_2$	−1785.035	0.008	0.002
	$^3B_1$	−1784.955	0.012	0.002
	$^3A_2$	−1784.843	−0.005	0.002
ROHF				
C_{2v}	$^3B_1$	−1785.340	−0.011	0.000

The D_3 isomer of C_{78} is one of the few higher fullerenes possessing non-Abelian symmetry. Its lowest triplet belongs to the A_2 irrep of the D_3 group (Table 6). The molecule preserves its symmetry as this state is a minimum on the energy surface. The T_1 energy is 0.903 eV, decreasing to 0.548 eV after relaxation. The bond lengths fall in the range of 1.401−1.450 Å in this state. Its zfs D is very close to that of C_{60}, and E is zero by symmetry. In Figure 3b the molecule is shown parallel to the C_3 axis. The spin density distribution is equatorial. The next two triplets are degenerate belonging to irrep E. The molecule distorts to C_2 group where the E irrep splits to the direct sum of irreps A and B. The A and B states are almost isoenergetic similarly to C_{70}. JT energies are close to those of C_{60} and C_{70}. Higher states do not sink below the lowest triplet due to the JT distortion. The spatial transition moment of the lowest triplet is nonzero. Though it is about twice as large as that of the third state, it is much smaller than that of the second one. Thus, triplet state properties are determined by the lowest one, and the triplet radiative dacay rate will be larger than that of C_{60} and C_{70}.

The lowest triplet of the C_{2v}-2 isomer lies 0.757 eV above the singlet ground state. This energy decreases to 0.426 eV when the geometry is allowed to relax. It belongs to the B_1 irrep and it is a minimum on the first triplet surface. Its bond lengths vary from 1.402 to 1.449 Å. The zfs D is almost equal to that of C_{60}. In Figure 3d the isomer can be seen perpendicular to the C_2 axis. The spin density distribution is similar to that of the C_{2v}-1 isomer. The transition moment of the lowest triplet is relatively large, but that of the next triplet is symmetry forbidden. Consequently, the lowest triplet may have quite short lifetime while the second one may be easier to see by experiment.

TABLE 8: Ground and Excited State Parameters for C_{82} (C_2-1)

group	state	total energy (eV)	D (cm^{-1})	E (cm^{-1})
ground state				
C_2	^{1}A	−1877.983		
CI				
C_2	^{3}B	−1877.458	−0.009	0.000
	^{2}B	−1876.949	−0.019	0.006
	^{3}A	−1876.893	−0.012	0.001
	^{3}B	−1876.697	−0.007	0.003
ROHF				
C_2	^{3}B	−1877.441	−0.005	0.000

TABLE 9: Ground and Excited State Parameters for C_{82} (C_2-2)

group	state	total energy (eV)	D (cm^{-1})	E (cm^{-1})
ground state				
C_2	^{1}A	−1877.939		
CI				
C_2	^{3}B	−1877.178	−0.008	0.001
	^{3}B	−1877.034	0.015	0.006
	^{3}B	−1876.806	−0.005	0.003
	^{3}A	−1876.753	−0.008	0.004
ROHF				
C_2	^{3}B	−1877.163	−0.004	0.001

TABLE 10: Ground and Excited State Parameters for C_{82} (C_2-3)

group	state	total energy (eV)	D (cm^{-1})	E (cm^{-1})
ground state				
C_2	^{1}A	−1877.273		
CI				
C_2	^{3}A	−1876.829	0.011	0.002
	^{3}B	−1876.908	0.009	0.003
	^{3}A	−1876.218	0.009	0.001
	^{3}A	−1876.093	0.004	0.001
ROHF				
C_2	^{3}A	−1876.816	0.009	0.004

We note that the difference between ROHF and CI-S results for the lowest triplet is negligible for all isomers indicating that the role of electron correlation is not substantial.

E. C_{82}. As the major component of the C_{82} mixture is one of the three C_2 symmetry isomers, we investigated these. To identify them, we applied the notation of ref 57: C_2-1, C_2-2, and C_2-3. We found that the relative stabilities are 0, 44, and 710 meV, respectively (see Tables 8−10). The ground state bond lengths varied between 1.397 and 1.457 (for C_2-1 and C_2-2), and 1.394 and 1.457 Å (for C_2-3). The lowest singlet excitation energies are 0.812, 1.022, and 0.656 eV, respectively. We have not found any data in the literature to compare with.

The lowest triplet energy of C_2-1 is 0.699 eV and decreases to 0.370 eV upon relaxation. It has symmetry B and it is a minimum on the lowest triplet surface. Bond lengths are in the range of 1.401−1.449 Å; that is, they span a slightly tighter interval than those in the ground state. The zfs D value is close to that of C_{60} (see Table 8). In Figure 3e the isomer is shown perpendicular to the C_2 axis. The spin density distribution is similar to that of C_{76}, the spins being small along the equator.

The T_1 energy of C_{82} (C_2-2) is 0.920 eV decreasing to 0.621 eV after relaxation. It has symmetry B and it is again a minimum on the surface. Its geometry can be characterized by bond lengths falling within 1.401−1.450 Å. The D value is close to that of C_{60} and C_{82} (C_2-1); see Table 9. In Figure 3f it can be seen perpendicular to the C_2 axis. The spin density distribution is similar to that of the previous isomer.

Among the fullerenes we investigated up to now, C_{82} (C_2-3) has the smallest T_1 energy: 0.514 eV (vertical) 0.309 eV (relaxed). It belongs to the totally symmetric irrep of C_2 and it is a minimum. Bond lengths are in the range of 1.400−1.454 Å in this state. The spin density distribution (Figure 3g) resembles that of the C_{2v} isomers of C_{78}. The absolute value of its D parameter is almost equal to that of C_{60} but it has the opposite sign.

TABLE 11: Ground and Excited State Parameters for C_{84} (D_{2d})

group	state	total energy (eV)	D (cm^{-1})	E (cm^{-1})
ground state				
D_{2d}	^{1}A$_1$	−1923.649		
CI				
C_{2v}[a]	^{3}A$_2$	−1922.743	0.017	0.004
D_{2d}	^{3}B$_1$	−1922.629	−0.015	0
	^{3}A$_2$	−1922.616	0.018	0
	^{3}A$_1$	−1922.524	−0.010	0
	^{3}B$_2$	−1922.516	−0.004	0
ROHF				
C_{2v}[a]	^{3}A$_2$	−1922.721	0.018	0.001

[a] Distorted state from the ^{3}B$_1$ parent representation, a saddle point in D_{2d}.

TABLE 12: Ground and Excited State Parameters for C_{84} (D_2)

group	state	total energy (eV)	D (cm^{-1})	E (cm^{-1})
ground state				
D_2	^{1}A$_1$	−1923.670		
CI				
C_2[a]	^{3}B	−1922.711	0.016	0.005
D_2	^{3}B$_3$	−1922.653	0.008	0.004
	^{3}B$_2$	−1922.590	0.018	0.002
	^{3}B$_3$	−1922.505	−0.002	0.001
	^{3}B$_2$	−1922.496	0.000	0.000
ROHF				
C_2[a]	^{3}B	−1922.690	0.015	0.002

[a] Distorted state from the ^{3}B$_3$ parent representation, a saddle point in D_2.

To the best of our knowledge it has not been decided which of the C_2 isomers is formed in the synthesis. We point out that zfs measurements can help to make a decision, as the D value of the C_2-3 isomer is quite different from that of the other two.

For two isomers (C_2-1 and C_2-2) we can see a significant discrepancy between ROHF and CI-S D values indicating a strong multiconfigurational character of the excited wave function thus a strong electron correlation in these systems. A common feature of all the three isomers is that they possess (i) quite small T_1 energies, and (ii) relatively large $T_1 \rightarrow S_0$ spatial transition moments. This latter point (ii) involves that the lifetime of the T_1 state should not be too long. However, (i) is interesting from another point of view: as the bimolecular rate constant of quenching of $^3C_{60}$ or some other molecule by fullerenes is proportional to the energy difference between the lowest triplets of the two molecules,[22] this rate constant should be the largest one for C_{82} isomers among the higher fullerenes studied here.

F. C_{84}. We performed calculations on the D_2-22 and D_{2d}-23 isomers (retaining the notation of ref 67) which were found to be the most probable candidates for the structure of C_{84}.[52,68−70] They will be referred to as D_2 and D_{2d}, respectively. Semiempirical tight-binding models revealed that the D_2 isomer is a little more stable than the D_{2d} one,[51,68] though an MNDO calculation states the opposite.[69] In our calculation the D_2 isomer turned out to be the more stable by 21 meV (Tables 11 and 12). The ground state bond lengths were in the range of 1.392−1.460 and 1.396−1.457 Å for D_{2d} and D_2 isomers, respectively. From the UV/vis spectrum[32,36] the excitation

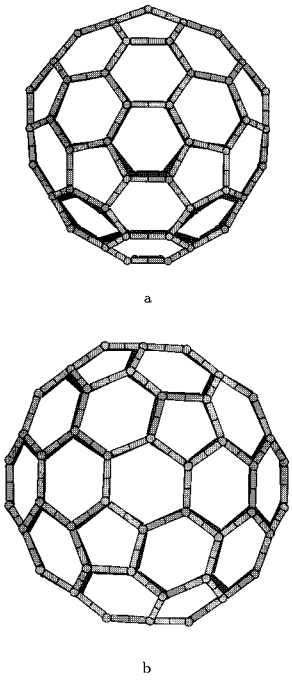

Figure 4. Spontaneous distortion of C_{84} isomers in lowest triplets. Distortions are magnified for visualization. (a) C_{84} (D_{2d}): distortion from D_{2d} $^3B_1$ (light) to C_{2v} $^3A_2$ state (dark). (b) C_{84} (D_2): distortion from D_2 $^3B_3$ (light) to C_2 ^3B state (dark).

energy of ground state−lowest singlet transition appears to be 1.2 eV. It was estimated as 1.3 eV for the D_{2d} and 1.2 eV for the D_2 isomer by tight-binding methods.[40] In our model the lowest singlet was estimated to lie at 1.27 eV for both the D_{2d} and D_2 isomers, in good agreement with the experiment and the other calculation.

D_{2d} is a non-Abelian group, so C_{84} can be a candidate for JT distortion. For C_{84}^- (D_{2d}) a JT distortion to C_2 was described.[28] The lowest four triplet states of the D_{2d} isomer belong to one-dimensional irreps. Thus, the molecule does not lose its symmetry by JT distortion in these states. Nevertheless, it distorts spontaneously. The situation is analogous to that of the benzene molecule. It has been known for a long time that benzene has D_{2h} symmetry in its first triplet in spite of belonging to a nondegenerate irrep in the D_{6h} group. A similar spontaneous distortion was predicted for the ground state of the C_{2v} isomer of C_{82}.[62] We observed the same type of distortion for the C_{84} isomers. The lowest triplet of the D_{2d} isomer has B_1 symmetry in D_{2d}. It lies by 1.129 eV above the ground state. However, it is a *saddle point* on the triplet surface, and, following the normal coordinate which corresponds to the negative eigenvalue of the Hessian, we arrive at the C_{2v} state. There are two almost isoenergetic C_{2v} minima belonging to A_2 irrep above the singlet ground state by 0.682 eV. These are included in Table 11 as the lowest triplets. The distortion energy, 115 meV, falls in the typical range of JT energies. Our calculations revealed that there is another saddle point between the two C_{2v} minima having C_2 symmetry[27] which may serve as the transition intermediate for a $C_{2v} \leftrightarrow C_{2v}$ motion. The bond lengths are between 1.404 and 1.447 Å in the D_{2d} B_1 saddle point and this interval increased to 1.392−1.461 Å upon distortion. The distortion is relatively large which is confirmed by the sign change of zfs D. The value of D is rather large among the fullerenes, and this holds also for the E parameter. A typical distortion is illustrated schematically in Figure 4a where the molecule is shown perpendicular to the main C_2 axis (the axis which is preserved in C_{2v}). Spin densities can be seen in Figure 3h; they are localized on one half of the molecule. The transition from C_{2v} A_2 to the ground state is spatially forbidden, so the molecule should have small radiative decay rate which was indeed observed experimentally (*vide infra*).

The D_2 isomer of C_{84} has a similar behavior. The first triplet has B_3 symmetry. Its excitation energy is 1.141 eV. This state is also a saddle point, and the molecule may distort to C_2 B state. This latter has an 0.77 eV phosphorescence energy (vertical transition at the C_2 geometry). Bond lengths are between 1.403 and 1.448 Å on the D_2 saddle and they changed to 1.397−1.458 Å as a consequence of the distortion. Direction of the distortion is identical to that of the other isomer but no so large which is indicated by the smaller distortion energy, 58 meV, and a smaller change in zfs D. The zfs parameters are quite large in comparison with other members of the fullerene family. There are two almost isoenergetic C_2 minima as in the case of the D_{2d} isomer and C_{70}. We found[27] that D_2 B_3 state is the lowest saddle point between the two minima. The $T_1 \rightarrow S_0$ transition has quite large spatial moment, and the lifetime of $^3C_{84}$ (D_2) cannot be too long. The triplet spectra of the C_{84} mixture is, therefore, probably determined by the D_{2d} isomer. In Figure 3i the molecule is shown perpendicular to the $C_2(z)$ axis. Spin densities are similar to those of the other isomer. In Figure 4b the distortion is demonstrated; the cluster can be seen parallel to the $C_2(z)$ axis which is preserved in C_2.

To the best of our knowledge, C_{84} is the only higher fullerene the triplet states of which were experimentally investigated.[18,19,22] Sauvé et al.[22] studied the triplet state of the mixture of the two isomers excited by biphenyl triplets in benzene. Direct excitation attempts by laser flash photolysis failed which was explained either by the low intersystem crossing efficiency or by the low extinction coefficient of the triplet state. The lifetime was estimated to be under 100 μs which is lower than that of C_{60} and C_{70}. They established that C_{84} can quench $^3C_{60}$ by triplet−triplet energy transfer. The lowest triplet of C_{60} was estimated to 1.6 eV,[6,7] so that of C_{84} must lie below this value which is in agreement with our calculations.

The only EPR experiment on higher fullerenes was performed by Boulas et al..[18,19] They investigated the electrochemistry and the EPR spectra of C_{84} anions. Both experiments confirmed the presence of two isomers. The EPR spectrum of the species generated in each redox step was measured and the species were assigned. The EPR spectrum of the doubly reduced mixture was studied in detail. It is known from theoretical investigations that the D_{2d} isomer has a doubly degenerate LUMO in contrast to the D_2 one which cannot have any degeneracy having Abelian symmetry. Thus, the EPR spectrum of C_{84}^{2-} can come from the lowest triplet of the D_{2d} isomer. From the temperature dependence of the EPR signal it was established that the lowest triplet is a thermally accessible state lying above the singlet ground state by 0.022 eV. The absolute value of the zero-field-splitting parameters were determined: $|D| = 0.001\,23$ cm^{-1} and $|E| = 0.000\,03$ cm^{-1}. To explain these experimental results we performed calculations on C_{84}^{2-} (D_{2d}). As the ground state of the ion is degenerate, we treated directly the triplet excited state at the ROHF level. The decomposition of the $E \otimes E$ direct product contains only one-dimensional irreducible representations: $A_1 \otimes A_2 \otimes B_1 \otimes B_2$. Thus, the ion preserves its symmetry and does not distort. This is in agreement with the very small value of E. Our zfs values are $D = -0.005$ and $E = 0.000$ cm^{-1} (note again that the errors of the calculated D values are usually in the third decimal).

TABLE 13: Predicted Zfs Values for the Molecules of Interest

molecule	group	state	D (cm^{-1})	E (cm^{-1})
C_{60}	D_{5d}	$^3A_{2g}$	−0.010	0
C_{70}	D_{5h}	$^3A'_2$	−0.002	0
C_{76}	D_2	$^3B_2$	−0.008	0.002
C_{78} (D_3)	D_3	$^3A_2$	−0.012	0
C_{78} (C_{2v}-1)	C_{2v}	$^3A_2$	0.020	0.000
C_{78} (C_{2v}-2)	C_{2v}	$^3B_1$	−0.010	0.001
		$^3A_2$	0.008	0.002
C_{82} (C_2-1)	C_2	^3B	−0.009	0.000
C_{82} (C_2-2)	C_2	^3B	−0.008	0.001
C_{82} (C_2-3)	C_2	^3A	0.011	0.002
C_{84} (D_{2d})	C_{2v}	$^3A_2$	0.017	0.004
C_{84} (D_2)	C_2	^3B	0.016	0.005

IV. Conclusion

In summarizing, we analyzed the energetics, geometry and zfs of higher fullerenes in their triplet states. The excitation energies of the lowest triplets are quite small. For the studied systems they vary between 0.5 and 1.1 eV for vertical transitions, in contrast to C_{60} and C_{70} whose triplet energies are at about 1.5 eV. It can be deduced from experimental data for C_{60}, C_{70}, and C_{84}^{2-} that with increasing number of the atoms the energy of the lowest triplet decreases. This is supported by our calculations for these three systems, but for other higher fullerenes this decrease is not so monotonic. The lowest triplets of the C_{82} isomers lie at significantly smaller energies than those of any other investigated fullerenes. In addition, the lowest triplet excitation energy can vary within a wide range for different isomers of a cluster with a given number of atoms, as in the case of C_{78}.

As to the change of molecular geometries upon excitation, a general trend can be observed: a small prolongation of the shortest C−C bond along with a considerable shortening of the longest ones. This latter change can be as large as 0.014 Å, as for C_{78} C_{2v}-2. Accordingly, we can conclude that the dispersion of bond lengths in the triplet excited states is smaller than in the ground state, which is an indication for the increase of electron conjugation upon excitation. The behavior of C_{84} is somewhat different: after spontaneous distortion the ground state bond length distributions are recovered for both isomers.

Electron correlation was shown to be qualitatively important in C_{60} and C_{82}, while it did not strongly affect the triplet spectra for other molecules.

The agreement between the computed and experimental zfs data is very good for C_{60}, while for C_{70} and C_{84}^{2-} we can say only that the zfs parameters are small. No experimental results are yet available for other systems. The computed data with the assignment of lowest-energy distorted structures are collected in Table 13. As the zfs parameters are very sensitive to the isomerization and the symmetry of the excited state, the calculated data presented in this work may offer some help in future characterization of higher fullerenes.

Acknowledgment. The authors are indebted to Á. Szabados for discussions and for reading the manuscript. Financial support from the Hungarian Research Fund, the Hungarian Ministry of Education, and the Hungarian Academy of Sciences is gratefully acknowledged (grant No. T021179-T023052, MKM-183/96, AKP 96/2-462).

References and Notes

(1) *The Fullerenes*; Kroto, H. W., Fischer, J. E., Cox, D. E., Eds.; Pergamon Press: Oxford, UK, 1993.

(2) *Electronic Properties of Fullerenes*; Kuzmany, H., Fink, J., Mehring, M., Roth, S., Eds.; Springer-Verlag, Berlin, 1993.

(3) *Progress in Fullerene Research*; Kuzmany, H., Fink, J., Mehring, M., Roth, S., Eds.; World Scientific: Singapore, 1994.

(4) Ebbesen, T. W.; Tanigaki, K.; Kuroshima, S. *Chem. Phys. Lett.* **1991**, *181*, 501.

(5) Sension, R. J.; Phillips, C. M.; Szarka, A. Z.; Romanov, W. J.; McGhie, A. R.; McCauley, J. P.; Smith, A. B.; Hochstrasser, R. M. *J. Phys. Chem.* **1991**, *95*, 6075.

(6) Lee, M.; Song, O.-K.; Seo, J.-C.; Kim, D.; Suh, Y. D.; Jin, S. M.; Kim, S. K. *Chem. Phys. Lett.* **1992**, *196*, 325.

(7) Dimitrijević, N. M.; Kamat, P. V. *J. Phys. Chem.* **1992**, *96*, 4811.

(8) Arbogast, J. W.; Darmanyan, A. P.; Foote, C. S.; Rubin, Y.; Diederich, F. N.; Alvarez, M. M.; Anz, S. J.; Whetten, R. L. *J. Phys. Chem.* **1991**, *95*, 11.

(9) Arbogast, J. W.; Foote, C. S. *J. Am. Chem. Soc.* **1991**, *113*, 8886.

(10) Tanigaki, K.; Ebbesen, T. W.; Kuroshima, S. *Chem. Phys. Lett.* **1991**, *185*, 189.

(11) Bensasson, R. V.; Hill, T.; Lambert, C.; Land, E. J.; Leach, S.; Truscott, T. G. *Chem. Phys. Lett.* **1993**, *206*, 197.

(12) Wasielewski, M. R.; O'Neil, M. P.; Lykke, K. R.; Pellin, M. J.; Gruen, D. M. *J. Am. Chem. Soc.* **1991**, *113*, 2774.

(13) Closs, G. L.; Gautam, P.; Zhang, D.; Krusic, P. J.; Hill, S. A.; Wasserman, E. *J. Phys. Chem.* **1992**, *96*, 5228.

(14) Bennati, M.; Grupp, A.; Mehring, M.; Dinse, K. P.; Fink, J. *Chem. Phys. Lett.* **1992**, *200*, 440.

(15) Bennati, M.; Grupp, A.; Mehring, M. *J. Chem. Phys.* **1995**, *102*, 9457.

(16) Bennati, M.; Grupp, A.; Mehring, M. In *Physics and Chemistry of Fullerenes and Derivatives*; Kuzmany, H., Fink, J., Mehring, M., Roth, S. World Scientific: Singapore, 1995; p 250.

(17) Terazima, M.; Hirota, N.; Shinohara, H.; Saito, Y. *Chem. Phys. Lett.* **1992**, *195*, 333.

(18) Boulas, P. L.; Jones, M. T.; Kadish, K. M.; Ruoff, R. S.; Lorents, D. C.; Tse, D. S. *J. Am. Chem. Soc.* **1994**, *116*, 9393.

(19) Boulas, P. L.; Jones, M. T.; Ruoff, R. S.; Lorents, D. C.; Malhotra, R.; Tse, D. S.; Kadish, K. M. *J. Phys. Chem.* **1996**, *100*, 7573.

(20) Bennati, M.; Grupp, A.; Mehring, M.; Dinse, K.; Fink, J. *Chem. Phys. Lett.* **1992**, *200*, 440.

(21) Regev, A.; Gamliel, D.; Meiklyar, V.; Michaeli, S.; Levanon, H. *J. Phys. Chem.* **1993**, *97*, 3671.

(22) Sauvé, G.; Kamat, P. V.; Ruoff, R. S. *J. Phys. Chem.* **1995**, *99*, 2162.

(23) Haufler, R. E.; Wang, L.-S.; Chibante, L. P. F.; Jin, C.; Conceicao, J.; Chai, Y.; Smalley, R. E. *Chem. Phys. Lett.* **1993**, *206*, 197.

(24) Surján, P. R.; Udvardi, L.; Németh, K. *J. Mol. Struct.* (THEOCHEM) **1994**, *311*, 55.

(25) Surján, P. R.; Németh, K.; Bennati, M.; Grupp, A.; Mehring, M. *Chem. Phys. Lett.* **1996**, *251*, 115.

(26) Németh, K.; Kállay, M.; Surján, P. R. In *Fullerenes and Fullerene Nanostructures*; Kuzmany, H., Fink, J., Mehring, M., Roth, S., Eds.; World Scientific: Singapore, 1996; p 372.

(27) Surján, P. R.; Kállay, M.; Dömötör, G.; Stachó, L.; Bán, M. In *Proceedings of International Winterschool on Electronic Properties of Novel Materials*; Kuzmany, H., Fink, J., Mehring, M., Roth, S., Eds.; World Scientific: Singapore, 1997; in press.

(28) Okada, M.; Okahara, K.; Tanaka, K.; Yamabe, T. *Chem. Phys. Lett.* **1993**, *209*, 91.

(29) Surján, P. R.; Németh, K.; Kállay, M. *J. Mol. Struct.* (THEOCHEM) **1997**, *398*, 293.

(30) Bendale, R. D.; Baker, J. D.; Zerner, M. C. *Int. J. Quantum. Chem.* **1991**, *S25*, 557.

(31) Kállay, M.; Németh, K.; Surján, P. R. *Fullerene Sci. Technol.* **1997**, *5*, 355.

(32) Diederich, F.; Ettl, R.; Rubin, Y.; Whetten, R. L.; Beck, R.; Alvarez, M.; Anz, S.; Sensharma, D.; Wudl, F.; Khemani, K. C.; Koch, A. *Science* **1991**, *252*, 548.

(33) Ettl, R.; Chao, I.; Diederich, F.; Whetten, R. L. *Nature (London)* **1991**, *353*, 149.

(34) Diederich, F.; Whetten, R. L.; Thilgen, C.; Ettl, R.; Chao, I.; Alvarez, M. *Science* **1991**, *254*, 1768.

(35) Hino, S.; Matsumoto, K.; Hasegawa, S.; Takahashi, T.; Seki, K.; Kikuchi, K.; Suzuki, S.; Ikemoto, I.; Achiba, Y. *Chem. Phys. Lett.* **1992**, *197*, 38.

(36) Hino, S.; Matsumoto, K.; Hasegawa, S.; Kamiya, K.; Inokuchi, H.; Morikawa, T.; Takahashi, T.; Seki, K.; Kikuchi, K.; Suzuki, S.; Ikemoto, I.; Achiba, Y. *Chem. Phys. Lett.* **1992**, *190*, 169.

(37) Benz, M.; Fanti, M.; Fowler, P. W.; Fuchs, D.; Kappes, M. M.; Michel, C. L. R. H.; Orlandi, G.; Zerbetto, F. *J. Phys. Chem.* **1996**, *100*, 13399.

(38) Orlandi, G.; Zerbetto, F.; Fowler, P. W.; Manolopoulos, D. E. *Chem. Phys. Lett.* **1993**, *208*, 441.

(39) Bendale, R. D.; Zerner, M. C. *J. Phys. Chem.* **1995**, *99*, 13830.

(40) Harigaya, K.; Abe, S. *J. Phys. Condens. Matter* **1996**, *8*, 8057.
(41) Fowler, P. W.; Batten, R. C.; Manolopoulos, D. E. *J. Chem. Soc., Faraday Trans.* **1991**, *87*, 3103.
(42) Manolopoulos, D. E.; Fowler, P. W. *J. Chem. Phys.* **1992**, *96*, 7603.
(43) Manolopoulos, D. E. *J. Chem. Soc., Faraday Trans.* **1991**, *87*, 2861.
(44) Manolopoulos, D. E.; May, J. C.; Down, S. E. *Chem. Phys. Lett.* **1981**, *181*, 105.
(45) Fowler, P. W. *J. Chem. Soc., Faraday Trans.* **1991**, *87*, 1945.
(46) Fowler, P. W.; Steer, J. I. *J. Chem. Soc. Chem. Commun.* **1987**, 1403.
(47) Fowler, P. W. *J. Chem. Soc., Faraday Trans.* **1990**, *86*, 2073.
(48) Ben-Amotz, D.; Cooks, R. G.; Dejarme, L.; Gunderson, J. C.; Hoke, S. H.; Kahr, B.; Payne, G. L.; Wood, J. M. *Chem. Phys. Lett.* **1991**, *183*, 149.
(49) Kikuchi, K.; N, N.; Wakabayashi, T.; Honda, M.; Matsumiya, H.; Morivaki, T.; Suzuki, S.; Shiromaru, H.; Saito, K.; Yamauchi, K.; Ikemoto, I.; Achiba, Y. *Chem. Phys. Lett.* **1992**, *188*, 177.
(50) Taylor, R.; Langley, G. J.; Avent, A. G.; Dennis, J. S.; Kroto, H. W.; Walton, D. R. M. *J. Chem. Soc. Perkin Trans. 2* **1993**, 1029.
(51) Zhang, B. L.; Wang, C. Z.; Ho, K. M. *Chem. Phys. Lett.* **1992**, *193*, 225.
(52) Zhang, B. L.; Wang, C. Z.; Ho, K. M.; Xu, C. H.; Chan, C. T. *J. Chem. Phys.* **1993**, *98*, 3095.
(53) Colt, J. R.; Scuseria, G. E. *J. Phys. Chem.* **1992**, *96*, 10265.
(54) Bakowies, D.; Gelessus, A.; Thiel, W. *Chem. Phys. Lett.* **1992**, *197*, 324.
(55) Raghavachari, K.; Rohlfing, C. M. *Chem. Phys. Lett.* **1993**, *208*, 436.
(56) Niles, J. C.; Wang, X. Q. *J. Chem. Phys.* **1995**, *103*, 7040.
(57) Kikuchi, K.; Nakahara, N.; Wakabayashi, T.; Suzuki, S.; Shiromaru, H.; Miyake, Y.; Saito, K.; Ikemoto, I.; Kainosho, M.; Achiba, Y. *Nature (London)* **1992**, *357*, 142.
(58) Taylor, R.; Langley, G. J.; Dennis, J. S.; Kroto, H. W.; Walton, D. R. M. *J. Chem. Soc. Chem. Commun.* **1992**, 1043.
(59) Wakabayashi, T.; Kikuchi, K.; Suzuki, S.; Shiromaru, H.; Achiba, Y. *J. Phys. Chem.* **1994**, *98*, 3090.
(60) Manolopoulos, D. E.; Fowler, P. W.; Ryan, R. P. *J. Chem. Soc., Faraday Trans.* **1992**, *88*, 1225.
(61) Stone, A. J.; Wells, D. J. *Chem. Phys. Lett.* **1986**, *128*, 501.
(62) Nagase, S.; Kobayashi, K.; Kato, T.; Achiba, Y. *Chem. Phys. Lett.* **1993**, *201*, 475.
(63) Manolopoulos, D. E.; Fowler, P. W. *Chem. Phys. Lett.* **1991**, *187*, 1.
(64) Negri, F.; Orlandi, G.; Zerbetto, F. *Chem. Phys. Lett.* **1992**, *189*, 495.
(65) Tsuzuki, S.; Tanabe, K. *Chem. Phys. Lett.* **1992**, *195*, 352.
(66) Raghavachari, K.; Rohlfing, C. M. *J. Phys. Chem.* **1991**, *95*, 5768.
(67) Fowler, P. W.; Manolopoulos, D. E.; Ryan, R. P. *J. Chem. Soc., Chem. Commun.* **1992**, *1992*, 408.
(68) Zhang, B. L.; Wang, C. Z.; Ho, K. M. *J. Chem. Phys.* **1992**, *96*, 7183.
(69) Raghavachari, K. *Chem. Phys. Lett.* **1992**, *190*, 397.
(70) Manolopoulos, D. E.; Fowler, P. W.; Taylor, R.; Kroto, H. W.; Walton, D. R. M. *J. Chem. Soc., Faraday Trans.* **1992**, *88*, 3117.
(71) Balch, A. L.; Ginwalla, A. S.; Lee, J. W.; Noll, B. C.; Olmstead, M. M. *J. Am. Chem. Soc.* **1994**, *116*, 2227.
(72) Surján, P. R.; Németh, K.; Bennati, M.; Grupp, A.; Mehring, M. *Chem. Phys. Lett.* **1996**, *251*, 115.
(73) Koga, N.; Morokuma, K. *Chem. Phys. Lett.* **1992**, *196*, 191.
(74) Choho, K.; Langenaeker, W.; de Woude, G. V.; Geerlings, P. *J. Mol. Struct.* (THEOCHEM) **1996**, *362*, 305.
(75) Cheng, H.-P.; Whetten, R. L. *Chem. Phys. Lett.* **1992**, *197*, 44.
(76) Negri, F.; Orlandi, G.; Zerbetto, F. *Chem. Phys. Lett.* **1988**, *144*, 31.
(77) Negri, F.; Orlandi, G.; Zerbetto, F. *J. Chem. Phys.* **1992**, *97*, 6496.
(78) Coulson, A.; Golobiewski, A. *Proc. R. Soc. (London)* **1961**, *78*, 1310.
(79) Fagerström, J.; Stafström, L. *Phys. Rev. B* **1993**, *48*, 11367.
(80) Su, W. P.; Schrieffer, J. R.; Heeger, A. J. *Phys. Rev. B* **1980**, *22*, 2099.
(81) Longuet-Higgins, H. C.; Salem, L. *Proc. R. Soc. (London)* **1959**, *251*, 172.
(82) Kürti, J.; Surján, P. R. *J. Chem. Phys.* **1990**, *92*, 3247.
(83) Kürti, J.; Surján, P. R.; Kertész, M. *J. Am. Chem. Soc.* **1991**, *113*, 9865.
(84) Haddon, R. C. *Chem. Phys. Lett.* **1986**, *125*, 231.
(85) Haddon, R. C.; Brus, L. E.; Ragvachari, K. *Chem. Phys. Lett.* **1986**, *131*, 165.
(86) László, I.; Udvardi, L. *J. Mol. Struct.* (THEOCHEM) **1989**, *183*, 271.
(87) Surján, P. R. *J. Mol. Struct.* (THEOCHEM) **1995**, *338*, 215.
(88) László, I.; Udvardi, L. *Int. J. Quantum. Chem.* **1992**, *42*, 1651.
(89) László, I.; Udvardi., L. *Chem. Phys. Lett.* **1987**, *136*, 418.
(90) László, I.; Udvardi, L. *J. Mol. Struct.* (THEOCHEM) **1987**, *183*, 271.
(91) Negri, F.; Orlandi, G.; Zerbetto, F. *Chem. Phys. Lett.* **1988**, *144*, 31.
(92) Haymet, A. D. J. *J. Am. Chem. Soc.* **1986**, *108*, 319.
(93) Roothaan, C. C. J. *Revs. Mod. Phys.* **1960**, *32*, 179.
(94) Löwdin, P.-O. *Phys. Rev.* **1955**, *97*, 1474; *Adv. Chem. Phys.* **1959**, *2*, 207.
(95) Jahn, J. A.; Teller, E. *Phys. Rev.* **1936**, *49*, 874.
(96) Jahn, J. A.; Teller, E. *Proc. R. Soc. (London)* **1937**, *A161*, 220.
(97) Ceulemans, A.; Beyens, D.; Vanquickenborne, L. G. *J. Am. Chem. Soc.* **1984**, *106*, 5824.
(98) Ceulemans, A. *J. Phys. Chem.* **1987**, *87*, 5374.
(99) Wasserman, E.; Snyder, L. C.; Yager, W. A. *J. Chem. Phys.* **1964**, *41*, 1763.
(100) Kooter, J. A.; van der Waals, J. H.; Knop, J. V. *Mol. Phys.* **1979**, *37*, 1015.
(101) Surján, P. R.; Németh, K. In *Progress in Fullerene Research*; Kuzmany, H., Fink, J., Mehring, M., Roth, S., Eds.; World Scientific: Singapore, 1995; p 116.
(102) Pople, J. A.; Beveridge, D. L., *Approximate Molecular Orbital Theory*; McGraw-Hill: New York, 1970.
(103) Godfrey, M.; Kern, C. W.; Karplus, M. *J. Chem. Phys.* **1966**, *44*, 4459.
(104) Brinen, J. S.; Orloff, M. K. *J. Chem. Phys.* **1966**, *45*, 4747.
(105) Hameka, H. F. *J. Phys. Chem.* **1959**, *31*, 315.
(106) Brandon, R. N.; Gerkin, R. E.; Hutchison, C. A. *J. Chem. Phys.* **1962**, *37*, 447.
(107) Bennati, M.; Németh, K.; Surján, P. R.; ; Mehring, M. *J. Chem. Phys.* **1996**, *105*, 4441.
(108) Optimized bond lengths, Cartesian coordinates, atomic spin density distributions of the systems studied in this paper are available upon sending an e-mail to kallay@para.chem.elte.hu or surjan@para.chem.elte.hu.
(109) Stachó, L. L.; Bán, M. I. *Theor. Chim. Acta* **1992**, *83*, 433; **1993**, *84*, 535; *J. Math. Chem.* **1992**, *11*, 405; **1995**, *17*, 377; *Comput. Chem.* **1993**, *17*, 21.
(110) Dömötör, G.; Bán, M. I.; Stachó, L. L. *J. Comput. Chem.* **1993**, *14*, 1491; **1996**, *17*, 289.
(111) Bán, M. I.; Dömötör, G.; Stachó, L. L. *J. Mol. Struct.* (THEOCHEM) **1994**, *311*, 29.
(112) van Wüllen, C. *Chem. Phys. Lett.* **1994**, *219*, 8.
(113) Scuseria, G. E. *Chem. Phys. Lett.* **1991**, *180*, 451.
(114) Baker, J.; Fowler, P. W.; Lazzeretti, P.; Malagoli, M.; Zanasi, R. *Chem. Phys. Lett.* **1991**, *184*, 182.
(115) Saito, S.; Oshiyama, A. *Phys. Rev. B* **1991**, *44*, 11532.
(116) Woo, S. J.; Kim, E.; Lee, Y. H. *Phys. Rev. B* **1993**, *47*, 6721.
(117) Feng, J.; Li, J.; Li, Z.; Zerner, M. C. *Int. J. Quantum. Chem.* **1991**, *39*, 331.
(118) Balasubramanian, K. *Chem. Phys. Lett.* **1993**, *206*, 210.
(119) Kertész, M. *Adv. Quantum Chem.* **1982**, *15*, 161.
(120) *Tables of Interatomic Distances and Configuration in Molecules and Ions*; Special Publication No. 18; The Chemical Society: London, 1965.
(121) Hiraya, A.; Shobatake, K. *J. Chem. Phys.* **1991**, *94*, 7700.
(122) Doering, J. P. *J. Phys. Chem.* **1969**, *51*, 2866.
(123) Aoyagi, M.; Osamura, Y.; Iwata, S. *J. Chem. Phys.* **1985**, *83*, 1140.
(124) Hasimoto, T.; Nakao, H.; Hirao, K. *J. Chem. Phys.* **1996**, *104*, 6244.
(125) Krätschmer, W.; Lamb, L. D.; Fostiropoulos, K.; Huffman, D. R. *Nature (London)* **1990**, *347*, 167.
(126) Capozzi, V.; Casamassima, G.; Lorusso, G.; Minafra, A.; Piccolo, R.; Trovato, T.; Valentini, A. *Synt. Met.* **1996**, *77*, 3.
(127) Abouf, R.; Pommier, J.; Cvejanovic, S. *Chem. Phys. Lett.* **1993**, *213*, 503.
(128) Bennati, M.; Grupp, A.; Bäuerle, P.; Mehring, M. *J. Phys. Chem.* **1996**, *100*, 2849.